https://doi.org/10.5194/wes-2023-104
Preprint. Discussion started: 9 October 2023

eawe european academy of wind energy
Open Access WIND ENERGY SCIENCE DISCUSSIONS

Machine Learning-Based Estimate of The Wind Speed Over Complex Terrain Using the LSTM Recurrent Neural Network

Cássia Maria Leme Beu[1,*] and Eduardo Landulfo[1,*]

[1]Instituto de Pesquisas Energéticas e Nucleares (IPEN), 2242 Prof. Lineu Prestes Av., São Paulo, Brazil
[*]These authors contributed equally to this work.

Correspondence: Cássia Beu (cassia.beu@gmail.com)

Abstract. Accurate estimate of the wind speed profile is crucial for a range of activities such as wind energy and aviation. The power law and the logarithmic-based profiles have been widely used as universal formulas to extrapolate the wind speed profile. However, these traditional methods have limitations in capturing the complexity of the wind flow, mainly over complex terrain. In recent years, the machine learning techniques have emerged as a promising tool for estimating the wind speed profiles. In this study, we used the Long Short-Term Memory (LSTM) Recurrent Neural Network and observational lidar datasets from three different sites over complex terrain to estimate the wind profile until 230 m. Our results showed that the LSTM outperformed the Power Law as the distance from the surface increased. The coefficient of determination (R^2) was greater than 90% until 100 m when the input dataset included only variables of 40 m height. However, the performance of the model improved when the 60 m wind speed was added to the input dataset. Furthermore, we found that the LSTM model trained on one site with 40 and 60 m observational data and applied to others sites also outperformed the Power Law. Our results show that the machine learning techniques, particularly LSTM, is a promising tool for accurately estimating the wind speed profiles over complex terrain, even for short observational campaigns.

1 Introduction

Machine learning techniques is increasingly being adopted as a powerful tool in environmental sciences. We see many examples of this method applied for different purposes to forecast meteorological variables and their derivative products. Musyimi et al. (2022) estimated the evapotranspiration for western Kenya with a Gradient Boosting Machine Model and remote sensing data. Using a semi-supervised learning, Jiang et al. (2022) forecasted the particulate matter ($PM_{2.5}$) concentration and its trend over the heavy industrial zone of Shenyang (China). Furthermore, the authors also found out the most influential features for the $PM_{2.5}$ concentration for short (1 hour) and long (6 and 24 hours) predictions. Focusing in improving the computational costs, Mustakim et al. (2022) applied the Neighborhood Component Analysis (NCA) to select the more relevant variables to their models. They concluded that a universal predictor with a uniform structure can be built at every monitoring station in Malaysia without having to perform a preliminary analysis to obtain the relevant input parameters for the air pollutant index prediction. Jesemann et al. (2022) emphasized the importance of adding time variables as input data in order to enable a recognition of temporal patterns, in their case, the NO^2 concentration in Hamburg (Germany).

https://doi.org/10.5194/wes-2023-104
Preprint. Discussion started: 9 October 2023

eawe european academy of wind energy
Open Access WIND ENERGY SCIENCE DISCUSSIONS

The use of the machine learning techniques is not restricted to the local or regional scales. Liu et al. (2022), for example, proposed a multi-level circulation pattern classification to identify large-scale weather or climate disaster events. The forecasting and monitoring disasters were also the subject of Soria-Ruiz et al. (2022). They got high performance by applying machine learning algorithms to remote sensing datasets to detect the recurrent floods over Gulf of Mexico coastline and the central and southeastern part of Mexico. Among the methods evaluated, Song and Wang (2020) concluded that the neural networks are superior to produce monthly wildfire predictions one year in advance, providing thus, a valuable information for long-range fire planning and management. Adding the Principal Component Analysis (PCA), Zhang et al. (2022) improved the accuracy for the visibility prediction at Sichuan (China). Among the six machine learning algorithms evaluated, they found out that the neural network performed best. Cheng and Tsai (2022) proposed a hybrid methodology based on variable selection and autoregressive distributed lag to forecast the pollutant concentrations, which improved the results when compared to the full and without lag dataset. The Support Vector Regression (SVR), that is a supervised algorithm, performed better than the other four algorithms tested. Those are only few examples of innovative works adopting the machine learning techniques in the environmental sciences.

Forecasting the wind speed through machine learning has also been the target of the researchers, mainly due of the wind energy market, since the short-term wind speed forecast is essential to enhance the production efficiency of the wind power farms. Due the random feature of the wind speed, advanced strategies have been proposed. Wang et al. (2021) showed that their multi-layer cooperative combined forecasting system, which is based on a novel adaptive weighting scheme, overcame the limitations of the current single and combined forecasting methods and provided a more accurate and stable forecast. In their review paper, Bali et al. (2019) analyzed some works produced during this century and concluded that the techniques for the wind speed forecast have limitations, as low efficiency and high computational cost. They suggested that to overcome some problems, the use of the Long-Short Term Memory (LSTM) can improve the wind speed prediction for the power generation. Tukur et al. (2022) analyzed works produced between 2010 and 2020 and concluded that ensemble and hybrid methods are reaching high accuracy, because they present more abilities to model complex functions than the linear models. They agreed with Bali et al. (2019) that the LSTM looks promising in forecasting the wind speed and still recommend that the adaptiveness of the hybrid models needs to be further researched. Dalton and Bekker (2022) showed the improvement when considering other meteorological variables into the modeling. Their results pointed to the vertical wind and divergence as important predictors to the wind speed. In this way, He et al. (2022) included the 2 m temperature and surface pressure to train their dual-attention mechanism multi-channel convolutional LSTM model with the ERA5 dataset to forecast the 10 m wind speed. Zhou et al. (2023) also used the ERA5 dataset to investigate the grid-to-site conversion models, considering the altitude, the land use and the seasonality effects. The deep learning models outperformed the linear interpolation and the regression models to estimate the 10 m wind speed. The aforementioned works briefly exemplify that efforts have been applied to the wind speed forecast theme, however, the methods to estimate its vertical profile are still limited.

According to Pintor et al. (2022), extrapolating the wind speed to higher heights is still a challenge and from the two most widely used methods (the power law and the logarithmic-based profile) they found out that the first one is more accurate for a wide variety of landscapes. Only recently, machine learning techniques have been used to forecast the wind speed profile.

https://doi.org/10.5194/wes-2023-104
Preprint. Discussion started: 9 October 2023

Türkan et al. (2016) evaluated seven different machine learning methods to estimate the 30 m wind speed at Kutahya (Turkey) and concluded that the SVR produced the most realistic results than the other six. Al-Shaikhi et al. (2022) proposed the Particle Swarm Optimization (PSO) with the LSTM method and compared their results with others optimization algorithms for an experiment carried out at Dhahran (Saudi Arabia). Their model needs at least four different levels of observational data as input. Following the same tendency, Nuha et al. (2022) proposed the Regularized Extreme Learning Machine (RELM) to extrapolate the wind speed to higher heights. With the same dataset of Dhahran, Mohandes and Rehman (2018) used the Restricted Boltzmann Machine (RBM) method and at least observations of four heights as input. They showed that their method improved the wind speed forecast. Bodini and Optis (2020a) and Bodini and Optis (2020b) demonstrated the superiority of the machine learning techniques over the power and logarithmic laws through the "round-robin" validation and highlighted the improvement of including observational data that capture the diurnal variability of the atmospheric boundary layer. They included the Obukhov length, Turbulence Kinetic Energy and time of the day, all of them measured at 4 m. Vassallo et al. (2020) also improved their results including meteorological variables to the input dataset of their Artificial Neural Networks (ANN) model, but they warn that excess information can confuse the model and inputting data should be cautiously analyzed. They emphasized the importance of normalizing the input data. Bodini and Optis (2020a) and Bodini and Optis (2020b) conducted their experiments over almost plain terrains (Great Plains – US) and stressed the need of performing the same kind of analysis to more complex terrains. To the best of our knowledge, the most of the studies on vertical wind speed extrapolation were conducted for plain terrains, except for Vassallo et al. (2020) that analyzed different surfaces.

2 Data and methods

2.1 The LSTM Recurrent Neural Network

The Recurrent Neural Networks (RNNs) are neural networks that take the output of one time step as input in the subsequent time step and then build a memory of time series events. The RNNs are specifically designed to work, learn and predict sequential data (Medsker and Jain, 1999). The Long Short-Term Memory (LSTM) is a type of RNN that is considered a state-of-art tool for processing sequential and temporal data nowadays. The main advantage of the LSTM over the others RNNs is that the presence of internal memory allows maintaining long-term dependencies, avoiding the vanishing or exploding gradient problems (Smagulova and James, 2019). This was done by introducing a forget gate into the standard recurrent sigma cell of the RNNs. The forget gate can decide what information will be discarded (Yu et al., 2019) and makes the LSTM system a robust model that compensates for the imperfections in the input data (Sherstinsky, 2020). The LSTM cells are mathematically expressed by:

https://doi.org/10.5194/wes-2023-104
Preprint. Discussion started: 9 October 2023

eawe european academy of wind energy
Open Access WIND ENERGY SCIENCE DISCUSSIONS

$$f_t = \sigma(W_{fh}h_{t-1} + W_{fx}x_t + b_f) \quad (1)$$

$$i_t = \sigma(W_{ih}h_{t-1} + W_{ix}x_t + b_i) \quad (2)$$

$$\tilde{c}_t = \tanh(W_{\tilde{c}h}h_{t-1} + W_{\tilde{c}x}x_t + b_{\tilde{c}}) \quad (3)$$

$$c_t = f_t.c_{t-1} + i_t.\tilde{c}_t \quad (4)$$

$$o_t = \sigma(W_{oh}h_{t-1} + W_{ox}x_t + b_o) \quad (5)$$

$$h_t = \sigma_t \tanh(c_t) \quad (6)$$

where x_t and h_t are the inputs and the recurrent information at time t; c_t is the cell state of the LSTM; f_t, i_t and o_t are the forget, input and output gates; W_f, W_i, $W_{\tilde{c}}$ and W_o are the weights; b is the bias, the operator '.' is the pointwise multiplication of two vectors.

We run the LSTM using the Keras library (version 2.9) from Python (version 3.8.16) through Colab (the Google Research's platform). The missing data were interpolated using the interpolate Pandas function and then data were normalized through the StandardScaler function from the Sklearn library (Pedregosa et al., 2011). We identified the optimal hyperparameters by using the Kerastuner (O'Malley et al., 2019) with the Hyperband algorithm. Table A1 exhibits the tuned hyperparameters for each experiment. We maintained the default configuration of Keras for the others LSTM arguments (Keras, 2023).

2.2 Doppler lidar

We employed the Windcube v2 Doppler lidar, from Leosphere, during the field campaigns at three different sites. For the Windcube v2 technical specifications, see Beu and Landulfo (2022). The information of the field campaigns are listed in Table 1. The lidar was set up for 12 levels, as follows: 40, 60, 80, 100, 120, 140, 160, 180, 200, 230, 260 and 290 m and to retrieve

Table 1. Information of the field campaigns

SITE	ALTITUDE(m)	COORDINATES	OBSERVATIONAL PERIOD
1	721	-23.6;-46.7	18/Sept/2015 to 10/Mar/2016 11/Oct/2016 to 31/Dec/2-16
2	4	-23.9;-46.7	11/Mar/2016 to 25/Aug/2016
3	590	-23.4;-47.6	26/Jul/2017 to 06/Aug/2018

information each 10 minutes. The Windcube v2 system automatically discards data that the Carrier-to-Noise (CNR) ratio is under -23 dB and we removed data that presented availability less than 80% over 10 minutes.

We considered the observed data at 40 m to estimate the wind speed at higher levels (from 60 until 230 m). Beyond the 10 min

https://doi.org/10.5194/wes-2023-104
Preprint. Discussion started: 9 October 2023

eawe european academy of wind energy
Open Access WIND ENERGY SCIENCE DISCUSSIONS

mean wind speed (v40), we also considered the wind direction (dir40), the hour, and the standard deviation of the horizontal (σu + σv) e vertical (σw) wind speed to forecast the wind speed at higher heights. With the wind speed standard deviation, we estimated the Turbulence Kinetic Energy (TKE), which is the sum of the wind speed variances (Stull, 1988) and is expressed by:

$$TKE = \frac{1}{2}(\sigma_u^2 + \sigma_v^2 + \sigma_w^2) \tag{7}$$

As already found out, including cyclical variables improves the wind speed forecast (Bodini and Optis, 2020a, b; Baquero et al., 2022). The diurnal cycle is a strong feature of the sites under research and we will discuss this further. Since surface observations are not available, the 40 m TKE could indirectly transmit information related to temperature and stability, improving the modelling with respect to diurnal variability. This step is referred to **Experiment 1**.

After, we also added the 60 m wind speed as input to forecast the levels above and it is referred to **Experiment 2**. Following the advice of Bodini and Optis (2020a) and Bodini and Optis (2020b), we conducted two more experiments (**Experiment 3** and **Experiment 4**) which consisted in applying a trained model to the other two sites.

2.3 The Power Law

According to Pintor et al. (2022), the Power Law (PL) is the simplest and generally the most effective way to extrapolate the wind speed. The PL is given by:

$$V = V_r(\frac{z}{z_r})^{\alpha} \tag{8}$$

where, V and V_r are the wind speed at height z and at reference height z_r, respectively. α is the wind shear coefficient. They remind that: $\alpha < 0.1$, corresponds to unstable conditions; $0.1 < \alpha < 0.2$ is typical of neutral profile and $\alpha > 0.2$ describe a stable atmosphere.

2.4 Evaluation

For evaluating the model performances, we chose the metrics that have typically been used in similar works.

- **Coefficient of determination** (R^2): The R^2 tells us how much the model differs from the original data and it is related to the correlation coefficient.

$$R^2 = 1 - \frac{\Sigma_{i=1}^{N}(y_i - \hat{y_i})^2}{\Sigma_{i=1}^{N}(y_i - \overline{y})^2} \tag{9}$$

- **Mean Squared Error (MSE)**:

$$MSE = \frac{1}{N}\Sigma_{i=1}^{N}(y_i - \hat{y_i})^2 \tag{10}$$

https://doi.org/10.5194/wes-2023-104
Preprint. Discussion started: 9 October 2023

eawe european academy of wind energy
Open Access WIND ENERGY SCIENCE DISCUSSIONS

· **Mean Absolute Error (MAE)**:

$$MAE = \frac{1}{N}\Sigma_{i=1}^{N}|y_i - \hat{y}_i| \tag{11}$$

· **Mean Absolute Percentage Error (MAPE)**:

$$MAPE = \frac{100\%}{N}\Sigma_{i=1}^{N}\frac{y_i - \hat{y}_i}{max(\epsilon, |y_i|)} \tag{12}$$

where y_i, $\overline{y}$ and $\hat{y}_i$ are: the actual value, the mean of the observed data and the predicted value. N is the total number of data points and ϵ is an arbitrarily small but strictly positive number to avoid undefined results when y_i is zero. Zhou et al. (2022) and Baquero et al. (2022) provide detailed explanations for those metrics.

2.5 Observational campaigns

The observational campaigns occurred along three years (Table 1) on the southeastern portion of Brazil (Fig. 1). The three sites are identified by the red pins and the numbers over the map. As we see, all of them are relatively close to the coastline. Despite the proximity among each other (see the description of Fig. 1), the surfaces are completely different, starting by the altitude (Table 1). Beyond the altitude, we also should consider the different surface roughness among the sites. The Site 1 is inside a Metropolitan Region (São Paulo city) which is characterized by a chaotic constructive pattern that mixes high buildings common to a big city and simple residences. This pattern results from the strong social difference of a densely populated city that grew disorderly.

The Site 2 is a coastal municipality called Cubatão and is characterized by the large number of industries, due to the Santos Harbor, which is the biggest harbor complex in Latin America. Beyond the industrial zone, Cubatão is surrounded by natural parks of the Atlantic Rain Forest (Morellato and Haddad, 2000), residential areas and a high mountain chain (called Serra do Mar) on its north boundary. At this point, Serra do Mar rises up abruptly more than 700 m over a horizontal distance of 5 km and looks like a big wall. Vieira and Gramani (2015) provide a technical description of the Cubatão and Serra do Mar features. Cubatão suffered in the past with serious consequences related to the health and environmental degradation due the pollution. The effects on health attracted attention by the middle of the 1970 decade due the high rates of deaths and congenital anomalies and were, by that time, largely published by the regional media. By that time, Cubatão received the title of "the most polluted city in the world" (Hogan, 1994). Besides the effects on health, the pollution also caused extreme negative impacts to the environment. The deforested areas became vulnerable to severe landslides, exposing to the risk the communities living in the foothills and hill slopes. The compilation done by Cabral et al. (2022) reveals that Cubatão had the highest number of debris-flows in Brazil during the last 100 years (nine events), causing 11 fatalities (deaths and missing people) and over US$ 73 million in economic losses. Those negative pollution consequences demanded actions to mitigate the impacts (Lemos, 1998). Since then, many researches have been conducted there.

The Site 3 (Iperó municipality) is more than 130 km away from the coast, as indicated by Fig. 1. It is inside a predominantly rural area and about 10 km away from the urban zone of the Sorocaba municipality. Another important characteristic of this Site

https://doi.org/10.5194/wes-2023-104
Preprint. Discussion started: 9 October 2023

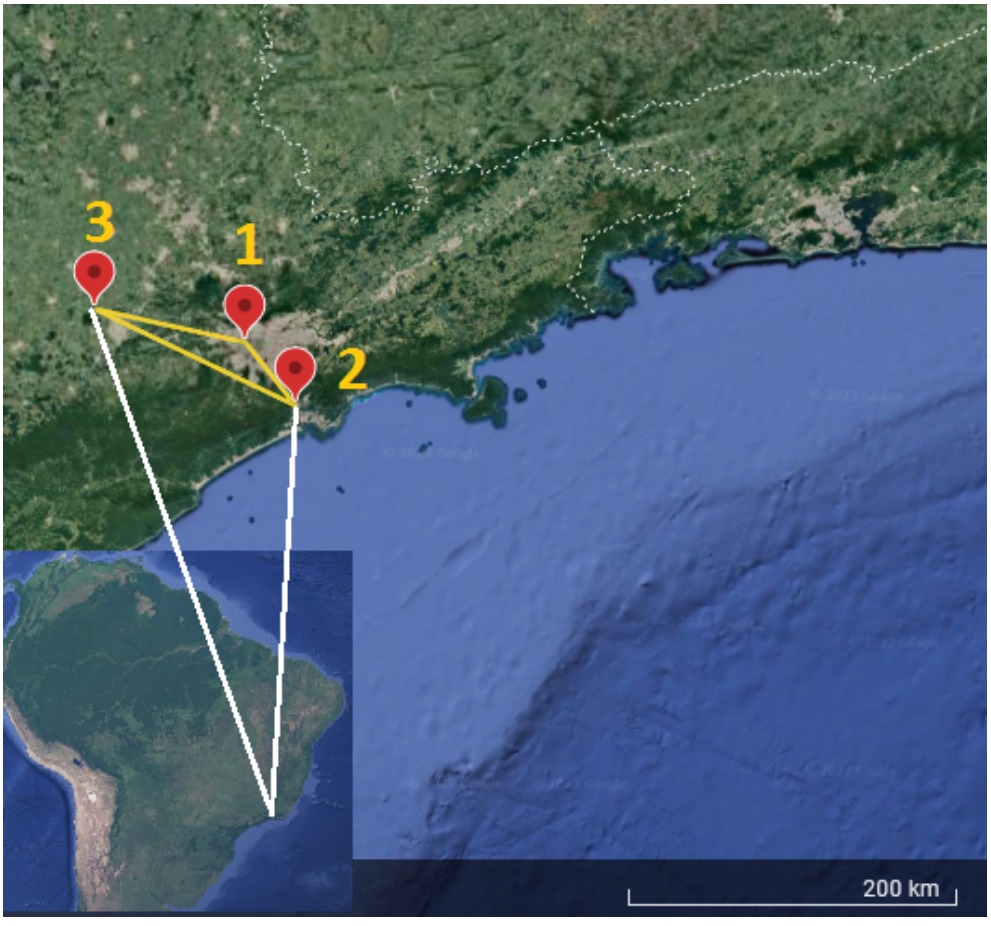

Figure 1. Sites of the observational campaigns. The distance (yellow line) is 47 km between Sites 1 and 2; 131 km between Sites 2 and 3; 90 km between Sites 1 and 3. Distance estimated by the © Google Earth tool.

is the Araçoiaba Hill, at its southeast boundary, that rises up more than 300 m, reaching more than 900 m above the sea level. The Araçoiaba Hill is inside a Federal Conservation Unit called Ipanema National Forest. Gasparoto et al. (2014) summarized some characteristics of the Ipanema National Forest.

3 Results

The surface strongly affects the atmospheric circulation within the Planetary Boundary Layer (PBL). Thus, we plotted the wind rose for the first observational level (40 m) as an attempt to identify similarities/differences among the three sites. The circulation patterns are similar between Sites 1 and 3 (Fig. 2 and Fig. 4). Both of them present a diurnal cycle of winds turning 360^o. The sea breeze (southeast wind) is one of the main reasons for this pattern at Site 1 (Ribeiro et al., 2018). According to Ribeiro et al. (2018), there are two main conditions that inhibit the sea breeze reaching the São Paulo Metropolitan Region

https://doi.org/10.5194/wes-2023-104
Preprint. Discussion started: 9 October 2023

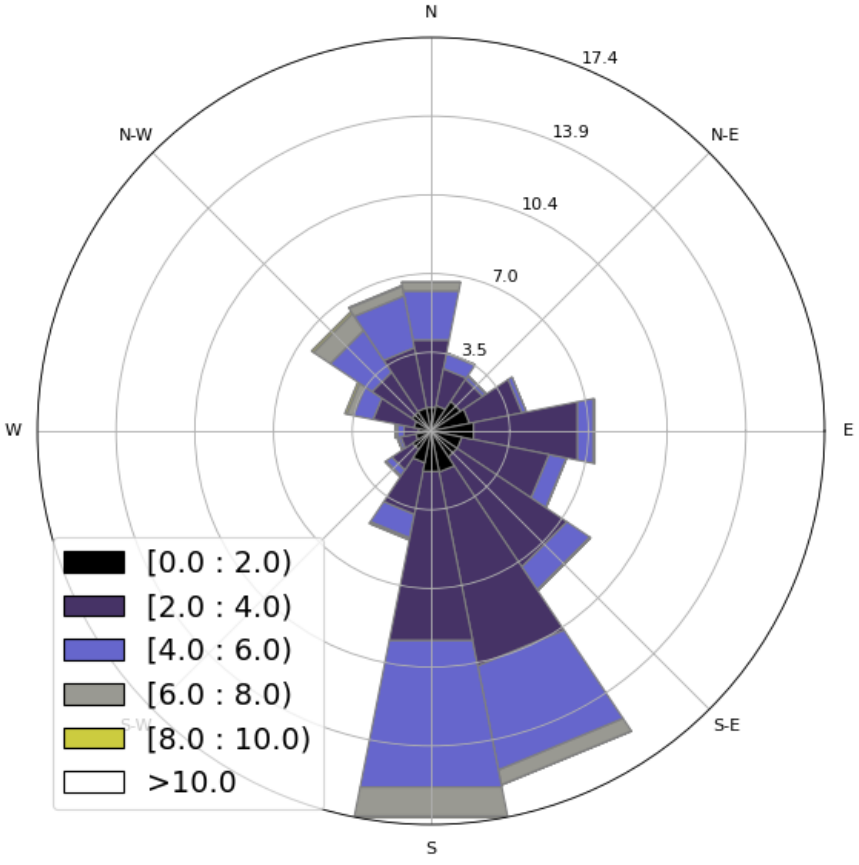

Figure 2. Observed wind at 40 m - Site 1 (normalized wind rose). The wind speed is indicated by legend (m s^{-1})

(SPMR): the prefrontal circulation and the cloudiness. The cloudiness decreases the thermal contrast between the sea and the land and the prefrontal circulation is opposed to the sea breeze. Thus, excluding those two conditions, the sea breeze advances over the SPMR often along the year and justifies the wind rose pattern (Fig. 2). Even at 40 m above the surface, the winds are weak and rarely reach 8 m/s. However, the Low-Level Jet (LLJ) is a typical feature of the SPMR (Sánchez et al., 2022).

At Site 2 (Fig. 3), it is also possible to identify a diurnal cycle, although, for this observational period, north and northeast winds were disproportionately more frequent than the other directions. Klockow and Targa (1998) illustrated a conceptual model (their Figure 2) and explained in a simplified way the local atmospheric circulation, where the sea and the land breezes play an important role. Compared to the Site 1, the wind speed is weaker. Vieira-Filho et al. (2015) also observed a similar pattern of Fig. 3 (rotating 360^o along the day) for the surface winds and emphasized the influences of the orography and the ocean on the local circulation. They detected around 20% of calms (wind speed < 1 m/s), occurring preferably at nighttime and

https://doi.org/10.5194/wes-2023-104
Preprint. Discussion started: 9 October 2023

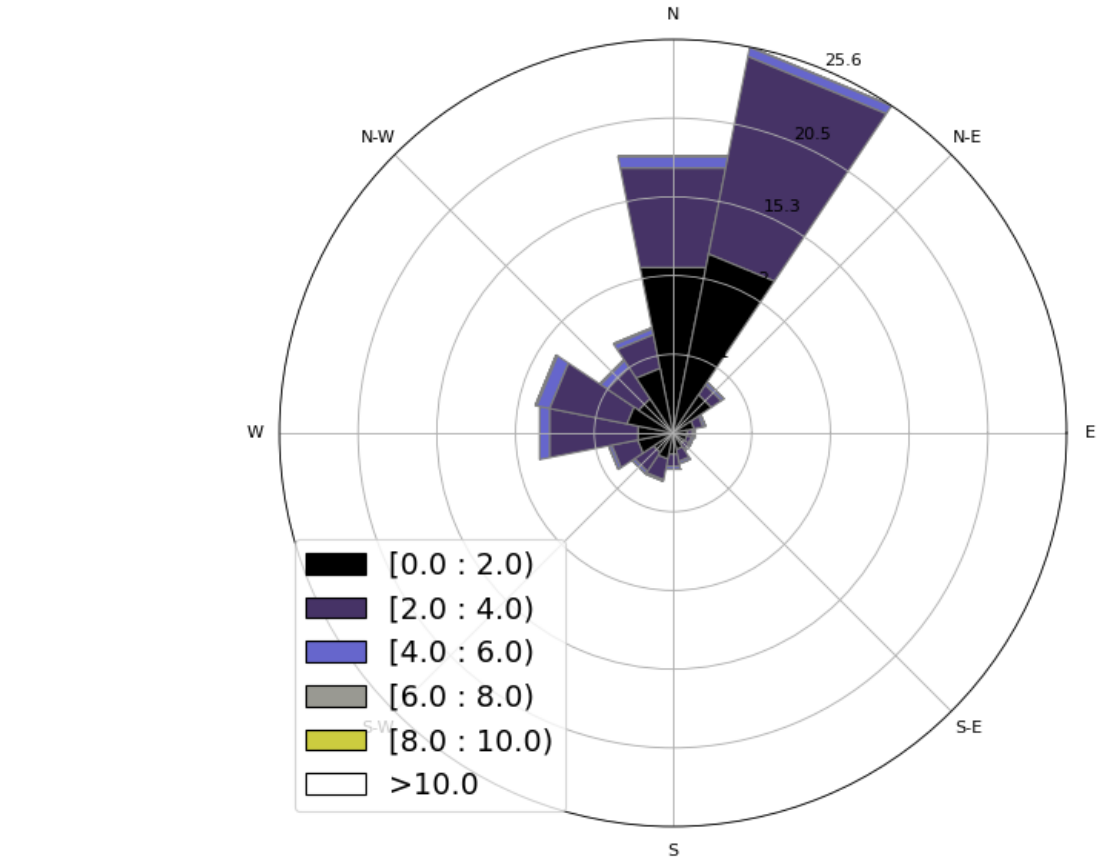

Figure 3. Observed wind at 40 m - Site 2 (normalized wind rose). The wind speed is indicated by legend (m s^{-1})

mean wind speed around 2.4 m/s.

The diurnal cycle at Site 3 (Fig. 4) is mainly related to the mountain-valley circulation since the valley (Tietê river valley) becomes deeper to northwest. Thus, the local circulation generally turns 360^o along the day. The circulation is also influenced by the frontal passages and the postfrontal condition generates stronger south and southeast winds than the prefrontal that generates weaker north and northwest winds. The LLJs are a recurrent feature observed at this Site (de Oliveira et al., 1995) and can form very near the surface (Beu and Landulfo, 2022). Winds are slightly stronger than the other two sites, but rarely reach 10 m/s (Fig. 4).

We carried out more than 60 experiments, testing different machine learning algorithms, size and type of inputs and tuning the models, until to reach the results that will be presented in this section. Although we will not show the results of those algorithms, it is worth mentioning that they were tested and discarded each time a better result was reached. We started our

https://doi.org/10.5194/wes-2023-104
Preprint. Discussion started: 9 October 2023

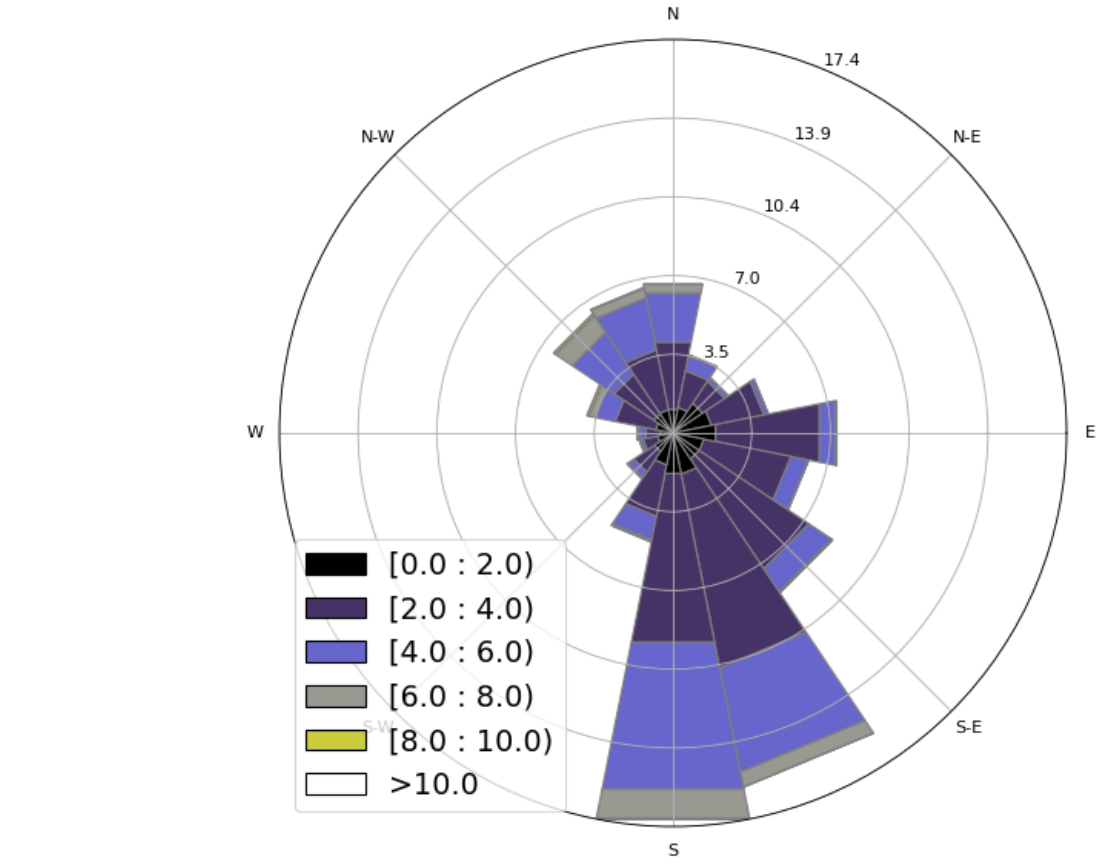

Figure 4. Observed wind at 40 m - Site 3 (normalized wind rose). The wind speed is indicated by legend (m s^{-1})

tests by the commonly used algorithms to forecast the wind speed, like: Random Forest Trees (Bodini and Optis, 2020a, b; Türkan et al., 2016), SVR (Türkan et al., 2016) and its two different implementations: nuSVR and LinearSVR (Pedregosa et al., 2011); the Multi-layer Perceptron (Türkan et al., 2016); and decomposition methods (Wang et al., 2021; Liu et al., 2022). Results also improved when 10 min mean data were used as input instead of 30 min mean or 1 hour mean. From this point, we refer to results with the LSTM RNN (Bali et al., 2019; Al-Shaikhi et al., 2022).

3.1 Experiment 1

We start to train our model with the Site 3 dataset, as machine learning generally requires large datasets, firstly providing only the wind speed at 40 m to forecast the wind speed at the higher heights. The entire dataset contains more than 50 thousand data for each variable. Thus, using the entire dataset for training and testing the model takes a while. Surprisingly, we found that the

https://doi.org/10.5194/wes-2023-104
Preprint. Discussion started: 9 October 2023

eawe european academy of wind energy
Open Access WIND ENERGY SCIENCE DISCUSSIONS

model only improves until a limited dataset size and was unnecessary to take the entire dataset. At each step, we evaluated the improvement through the metrics (Eq. 9 to 12).

For the Site 3, we found that the ideal dataset size was 8 thousand points, taking 90% for the training. Considering that our temporal series is composed of 10-min mean, this corresponds roughly to a two months of observational data. This means that a short observational campaign can produce reliable results. We followed testing the inclusion of other variables, as: wind direction, hour and TKE (Eq. 7), because those data give information about the diurnal cycle and improved the model. The tables 2, 3 and 4 present the results reached by the LSTM model and the Power Law (PL), according to Eq. 8 and $\alpha = 0.25$, as we found that this value provides the best correlation for our datasets. See Table A1 for the dataset sizes and hyperparameters. As we see, for the three sites, the R^2 is similar for estimates with the PL and the LSTM at the first level (60 m) however, as the distance from the surface increases, the LSTM estimates outperform the PL. This happens because the PL has a universal nature and cannot simulate features as the LLJ (Bodini and Optis, 2020a).

Table 2. Site 1 - Assessment of the wind speed estimated by the PL and the LSTM model (**Experiment 1**) until 230 m

Height (m)	Observed mean wind speed (m s^{-1})	Model	R^2	MSE (m s^{-1})	MAE (m s^{-1})	MAPE (%)
60	3.61	PL	0.98	0.06	0.20	6.47
		LSTM	0.98	0.05	0.17	6.63
80	3.85	PL	0.94	0.18	0.33	10.74
		LSTM	0.95	0.13	0.28	10.20
100	4.01	PL	0.90	0.30	0.43	13.06
		LSTM	0.93	0.21	0.35	11.43
120	4.17	PL	0.86	0.45	0.53	15.06
		LSTM	0.91	0.31	0.43	13.15
140	4.29	PL	0.82	0.62	0.62	17.08
		LSTM	0.88	0.41	0.50	14.64
160	4.41	PL	0.76	0.82	0.72	19.32
		LSTM	0.84	0.53	0.57	16.23
180	4.52	PL	0.69	1.07	0.82	21.71
		LSTM	0.81	0.66	0.63	18.17
200	4.64	PL	0.60	1.39	0.93	24.31
		LSTM	0.76	0.83	0.70	19.80
230	4.75	PL	0.48	1.86	1.08	28.19
		LSTM	0.70	1.05	0.78	22.96

https://doi.org/10.5194/wes-2023-104
Preprint. Discussion started: 9 October 2023

eawe european academy of wind energy
Open Access WIND ENERGY SCIENCE DISCUSSIONS

Table 3. Site 2 - Assessment of the wind speed estimated by the PL and the LSTM model (**Experiment 1**) until 230 m

Height (m)	Observed mean wind speed (m s^{-1})	Model	R^2	MSE (m s^{-1})	MAE (m s^{-1})	MAPE (%)
60	2.30	PL	0.96	0.09	0.21	12.8
		LSTM	0.97	0.08	0.20	12.6
80	2.50	PL	0.89	0.36	0.41	22.6
		LSTM	0.93	0.22	0.35	20.7
100	2.69	PL	0.81	0.88	0.60	30.3
		LSTM	0.91	0.43	0.46	26.1
120	2.91	PL	0.72	1.83	0.81	36.7
		LSTM	0.88	0.77	0.59	28.5
140	3.15	PL	0.65	3.08	1.01	41.7
		LSTM	0.89	0.97	0.66	29.4
160	3.35	PL	0.61	4.23	1.17	46.2
		LSTM	0.88	1.27	0.74	31.7
180	3.52	PL	0.58	5.11	1.31	49.8
		LSTM	0.89	1.39	0.79	33.8
200	3.70	PL	0.53	6.61	1.47	52.6
		LSTM	0.86	2.02	0.88	36.4
230	3.86	PL	0.50	7.79	1.61	55.3
		LSTM	0.80	3.04	1.05	38.1

For the Site 1, we reached the best result with a temporal series with 10 thousand points. This is approximately a 70 days observational campaign. When only 40 m variables are used as predictors, we obtain $R^2 > 90\%$ until 120 m. Observe that the PL performance decreases faster at Site 3 than at Site 1 (see Fig. 5 and Fig. 7). The MSE, MAE and MAPE also confirm the superiority of the LSTM model over the PL. We see from Fig. 5, 6 and 7 that the PL works better close to the surface. At 60 m, the PL performance compares to the LSTM (Fig. 8), but at 230 m, we see stronger winds underestimated by the PL (the red circle on Fig. 9).

The Site 2, which has weaker winds (see Table 3, column 2), presents better performance for the LSTM forecast from 140 m upwards than the other two sites. As shown by Fig. 6, R^2 remains almost constant above 140 m, while for the PL, the R^2 decreases faster than the Site 1 curve. The PL underestimates winds stronger than 8 m/s as illustrated by the scatter plot (Fig. 10) and are associated with abrupt changes as indicated by the temporal series (Fig. 11). The causes of that strengthening of the wind profile are unknown and remain as suggestion for a future investigation. The LSTM also underestimates the stronger

https://doi.org/10.5194/wes-2023-104
Preprint. Discussion started: 9 October 2023

eawe european academy of wind energy
Open Access WIND ENERGY SCIENCE DISCUSSIONS

Table 4. Site 3 - Assessment of the wind speed estimated by the PL and the LSTM model (**Experiment 1**) until 230 m

Height (m)	Observed mean wind speed (m s^{-1})	Model	R^2	MSE (m s^{-1})	MAE (m s^{-1})	MAPE (%)
60	4.59	PL	0.96	0.22	0.36	10.0
		LSTM	0.98	0.09	0.22	7.1
80	5.03	PL	0.89	0.64	0.62	14.9
		LSTM	0.96	0.21	0.34	10.0
100	5.37	PL	0.83	1.10	0.83	18.1
		LSTM	0.95	0.34	0.44	11.8
120	5.68	PL	0.77	1.64	1.01	20.8
		LSTM	0.92	0.60	0.58	13.6
140	5.93	PL	0.71	2.21	1.16	22.8
		LSTM	0.89	0.81	0.67	14.5
160	6.16	PL	0.62	2.94	1.33	25.1
		LSTM	0.86	1.11	0.78	15.4
180	6.36	PL	0.54	3.67	1.48	27.0
		LSTM	0.83	1.39	0.90	17.5
200	6.52	PL	0.47	4.33	1.61	28.7
		LSTM	0.80	1.66	0.97	18.5
230	6.75	PL	0.37	5.35	1.79	30.9
		LSTM	0.78	1.83	1.04	19.3

winds (mainly the winds that exceed 12 m/s), as we see from the scatter plot, but it captures the pattern better than the PL (Fig. 11).

The metrics show a similar behavior between Site 1 and Site 3. Despite the complex topography, perhaps the better performance of the LSTM model for the Site 2 for the levels above 140 m is related to the absence of the LLJ. To the best of our knowledge, LLJs so close to the surface have not been reported there yet; on the contrary, they are a common feature of the Sites 1 and 3 (Sánchez et al., 2022; de Oliveira et al., 1995; Beu and Landulfo, 2022).

3.2 Experiment 2

Some studies already showed that adding input variables from different heights below the extrapolation height improves the machine learning performances (Vassallo et al., 2020; Mohandes and Rehman, 2018). Thus, we added the 60 m wind speed observations to the input dataset of the experiment 1 to estimate the above heights. Adding the 60 m wind speed observations

https://doi.org/10.5194/wes-2023-104
Preprint. Discussion started: 9 October 2023

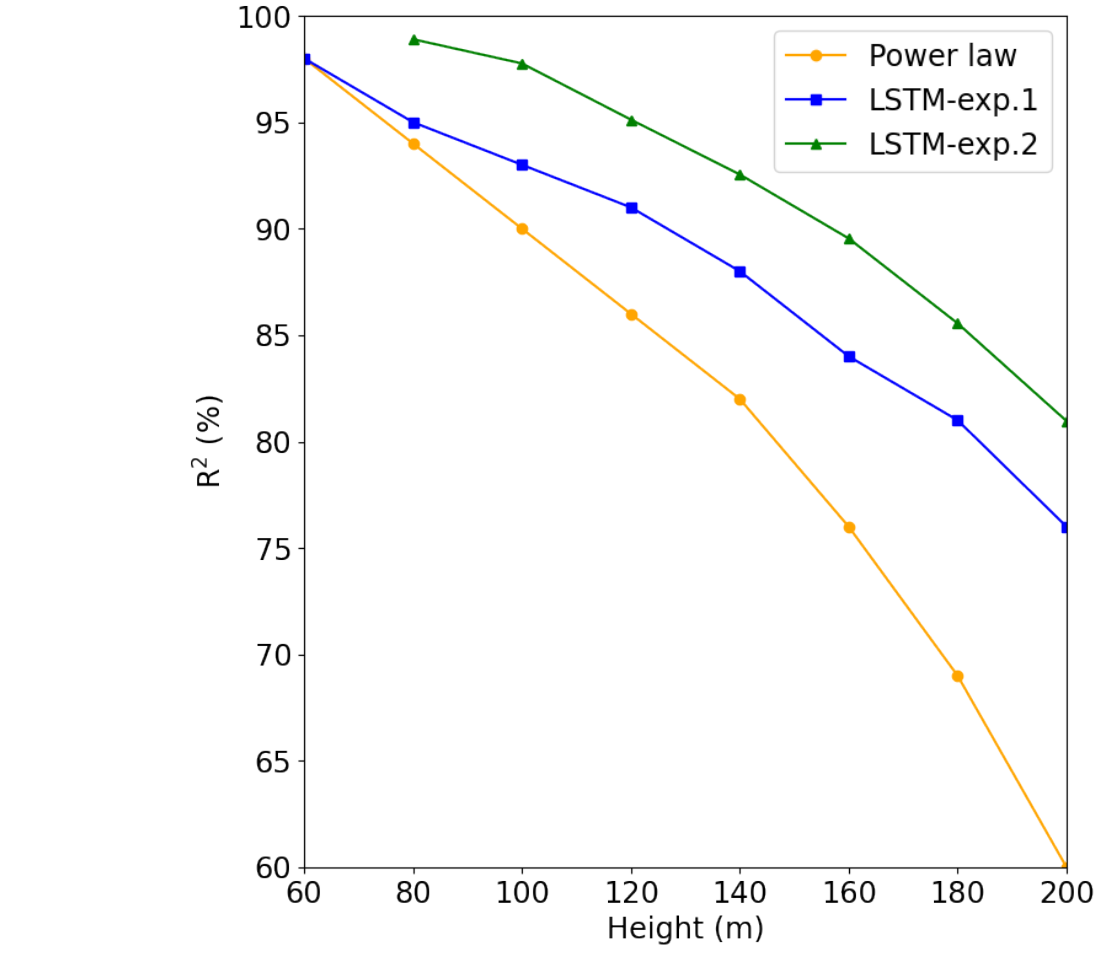

Figure 5. LSTM and Power Law R^2 estimates: Site 1. Exp.1 and exp.2 stand for experiment 1 and experiment 2, respectively

to the input dataset improved the results, as we see in Fig. 5, 6 and 7 (green line). For the Site 1 we see an increasing along the entire R^2 curve, reaching 99% at 80 m, while the MAE decreased by 50%. At 200 m, the R^2 increased by 6% and the MAE reduced more than 8%. The improvement was more pronounced at the lower heights for the Site 2 (compare the blue and green lines in Fig. 6). The R^2 increased to 98% against the 93% from Experiment 1 at 80 m and the MAPE was reduced by 70%, but for the higher levels, the improvement gradually decreases, as we see from Fig. 6.

For the Site 3, the Experiment 2 also outperformed the Experiment 1 and the improvement is constant with the height, just

https://doi.org/10.5194/wes-2023-104
Preprint. Discussion started: 9 October 2023

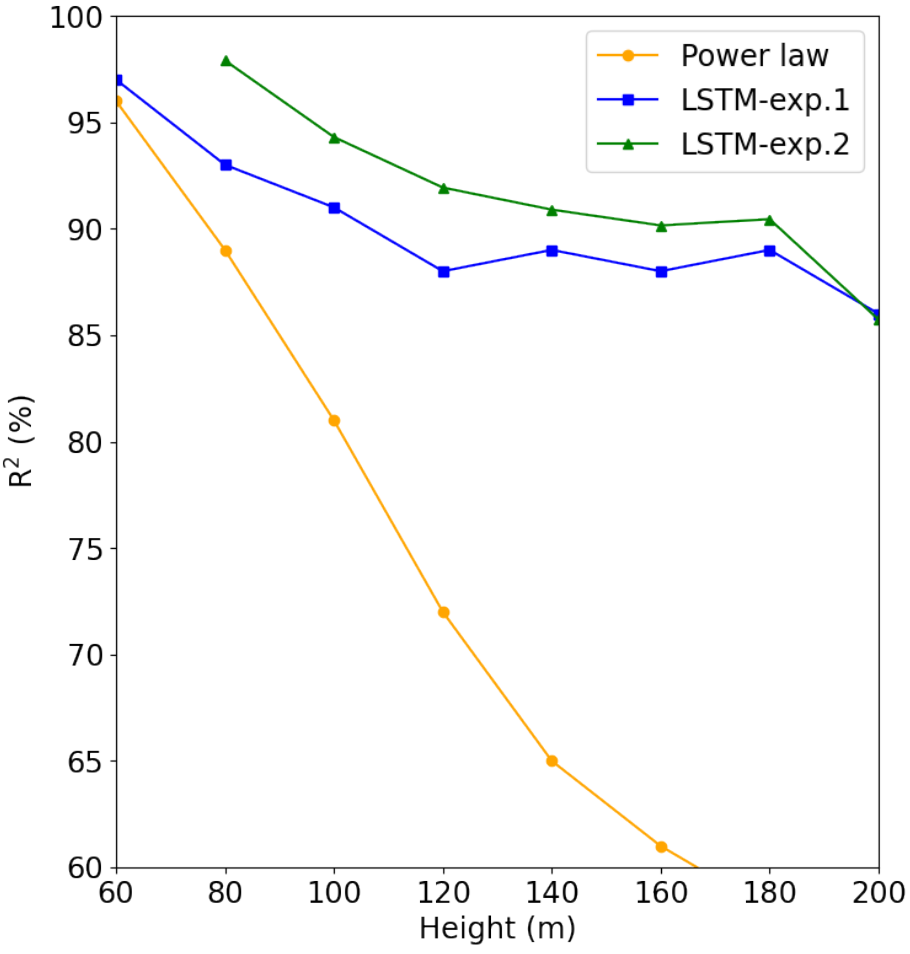

Figure 6. LSTM and Power Law R^2 estimates: Site 2. Exp.1 and exp.2 stand for experiment 1 and experiment 2, respectively

slightly better at 80 m as we see from the greater distance between the green and blue lines (Fig. 7). The R^2 increased 2.5% at 80 m and only 1.5% at 200 m.

3.3 Experiment 3

Bodini and Optis (2020b) advised about the importance of applying the machine learning models to different sites of that where they were trained. Following their advice, we applied each trained model to the other two sites (Fig. 12 - Fig. 14).

For the Site 1 (Fig. 12) we see that the Site 3 model (blue line) performed better than the Site 2 model (green line), but its

https://doi.org/10.5194/wes-2023-104
Preprint. Discussion started: 9 October 2023

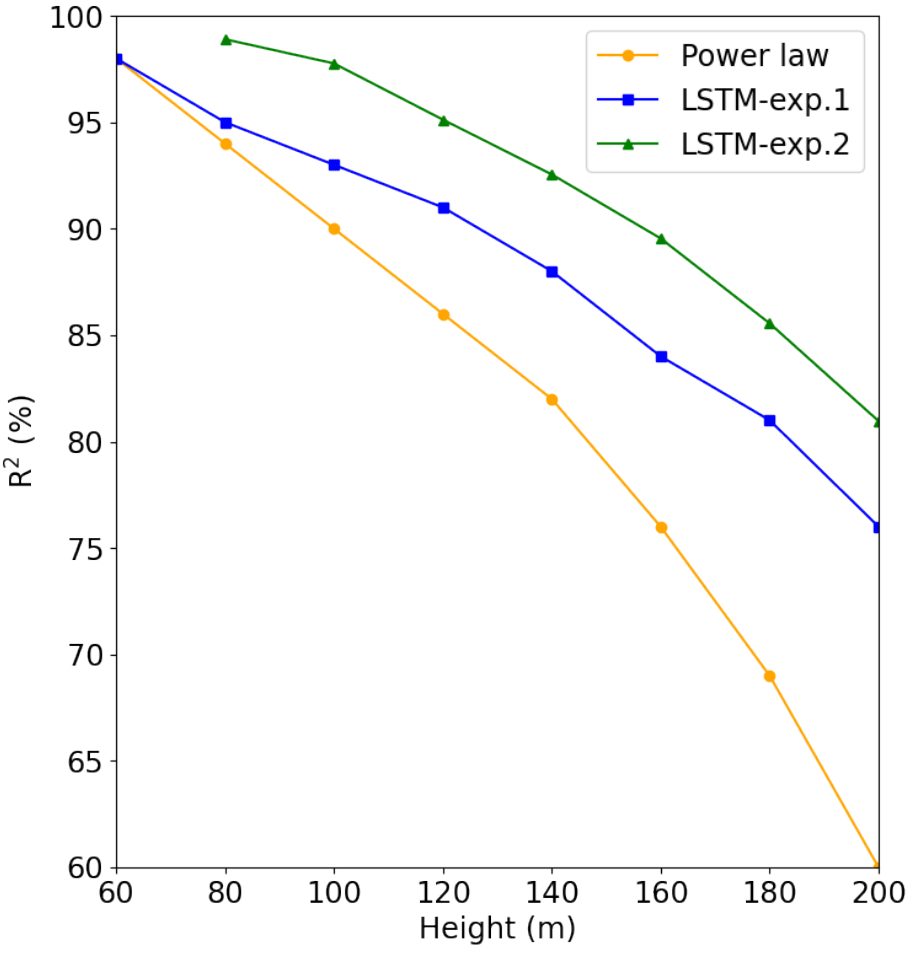

Figure 7. LSTM and Power Law R^2 estimates: Site 3. Exp.1 and exp.2 stand for experiment 1 and experiment 2, respectively

performance was worse than the original model (S1, that was trained and validated at the Site 1). It is also clear from this figure that the performance quickly decreases with the height. The behavior is the same for the Site 3 (Fig. 14), where the model trained for the Site 2 presented the worst result. The tests of the models trained at Site 1 and Site 3 for the Site 2 presented poor performance as indicated by the fast R^2 reduction with the height (Fig. 13).

Figures 15 - 17 show the correlation between observed and forecasted wind speed for 80 m, 100 and 140 m for the forecast of the Site 1 with the model trained at Site 3.

https://doi.org/10.5194/wes-2023-104
Preprint. Discussion started: 9 October 2023

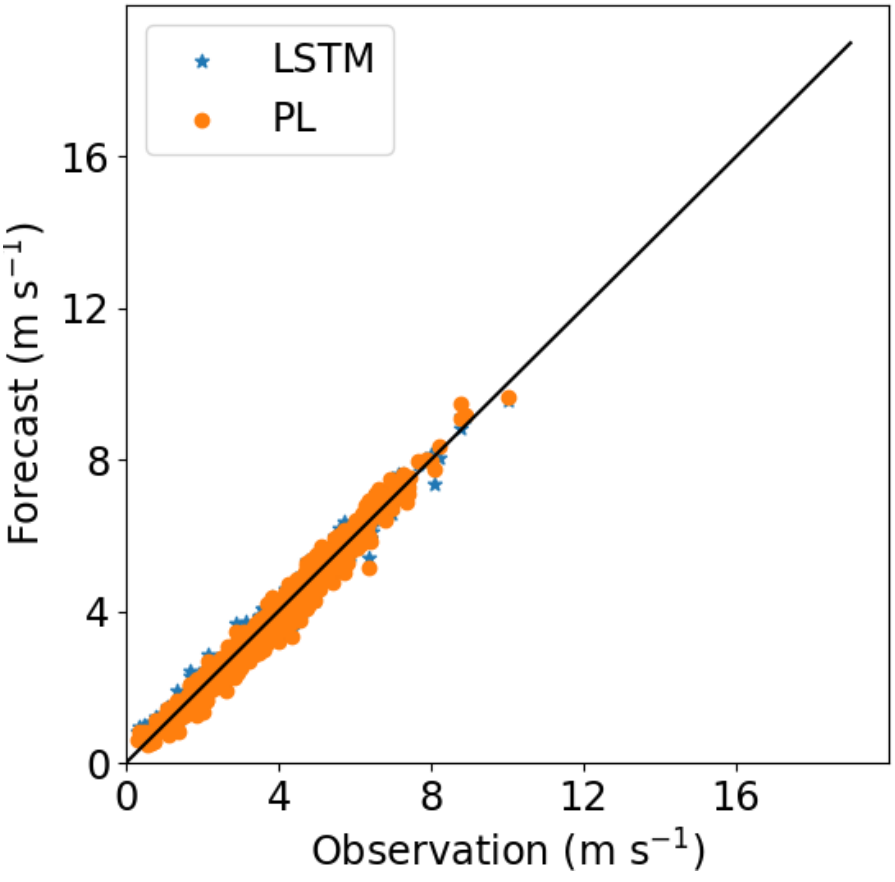

Figure 8. LSTM and PL forecasts (Site 3) for 60 m – results from **Experiment 1**

3.4 Experiment 4

For this step, we took the best result from the previous experiment (**Experiment 3**) and added the 60 m wind speed to the input dataset. That means, for the Site 1 case, took the model trained at Site 3.

The forecast for the Site 1 highly improves when the 60 m wind speed is included on the input dataset for training the model at Site 3, as we see in Fig. 18 and outperforms the PL forecast. The R^2 increased by 7% if compared with the LSTM forecast with only the 40 m observations (**Experiment 3**) for the 80 m height. The R^2 reached 90.6% and 84.9% at 120 and 140 m, respectively. This result is almost as good as **Experiment 1**. Figures 21 - 23 illustrate the improvement (compared to Fig. 15 - 17) when the 60 m wind speed observation was added to the training phase.

We also observe a strong improvement for the Site 3 (Fig. 20) compared to the PL estimate. At 80 m, the R^2 increased by 9%

https://doi.org/10.5194/wes-2023-104
Preprint. Discussion started: 9 October 2023

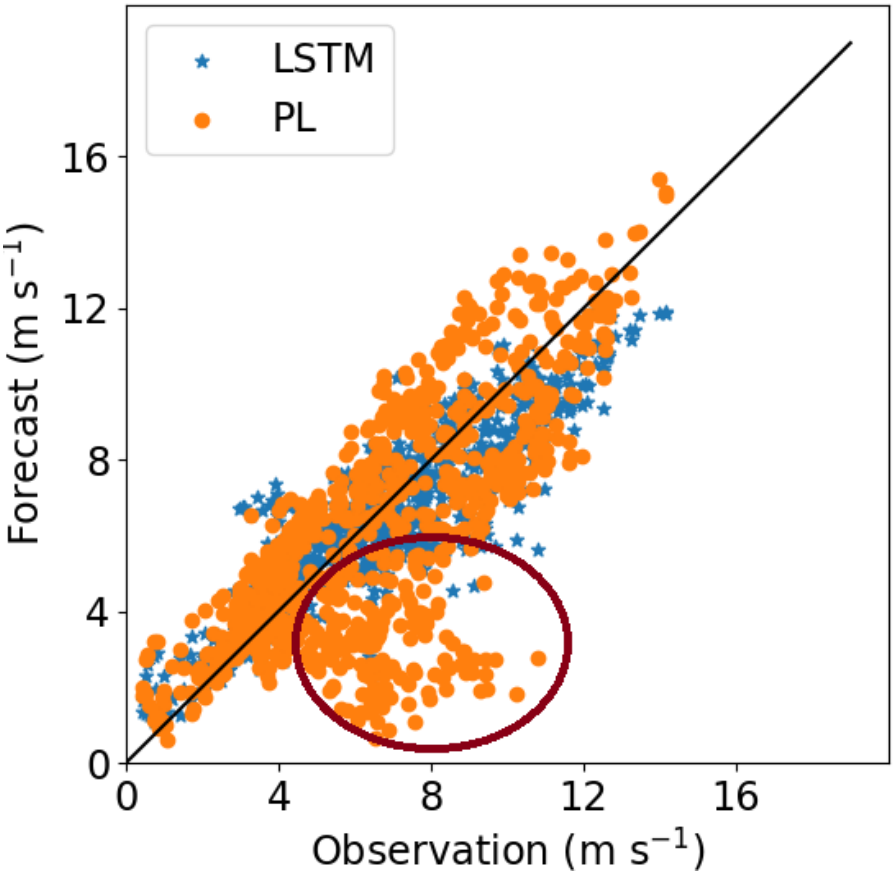

Figure 9. LSTM and PL forecasts (Site 3) for 230 m – results from **Experiment 1**

compared to the PL estimate, while at 140 m, we observed an increase of 16%.

For the Site 2 we used the model trained at Site 1, since that one performed best, as indicated by Fig. 13. In this case, we see improvement until 120 m (Fig. 19), but it was lesser than the other two cases. It is obvious that adding more observational levels to the input dataset would improve the results, however, it is not clear if this method should be applied if the surfaces are too different as the Site 2 in relation to Site 1 and Site 3. We recommend more tests for the complex terrain scenarios.

https://doi.org/10.5194/wes-2023-104
Preprint. Discussion started: 9 October 2023

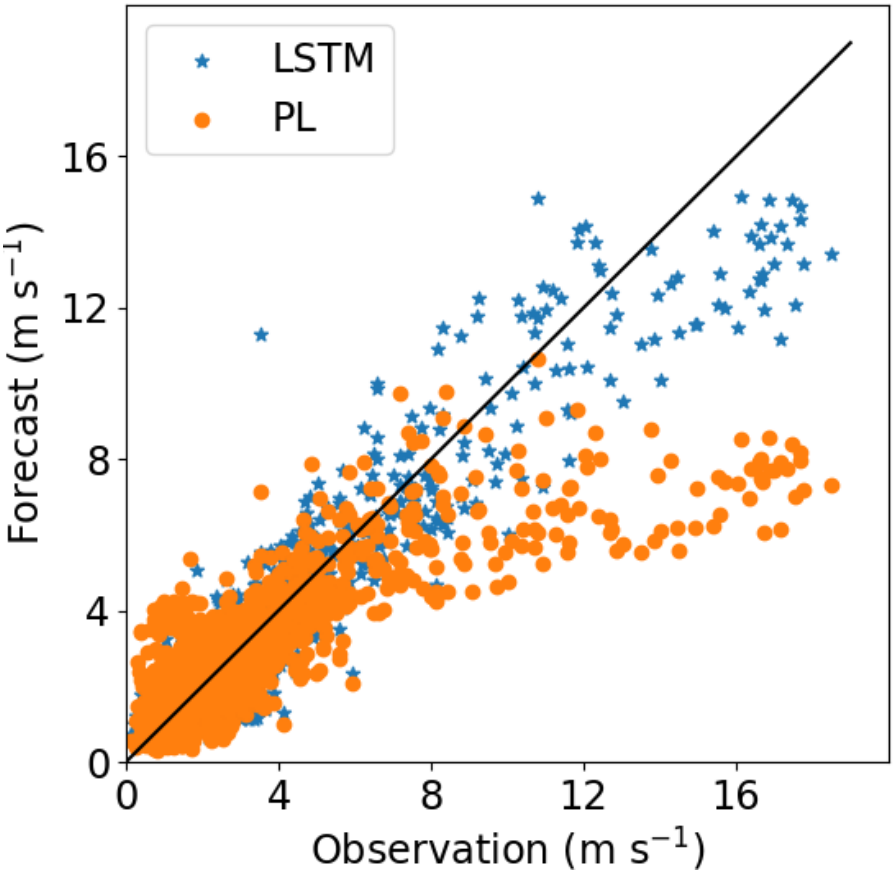

Figure 10. Site 2: 160 m wind speed forecast (**Experiment 1**)

https://doi.org/10.5194/wes-2023-104
Preprint. Discussion started: 9 October 2023

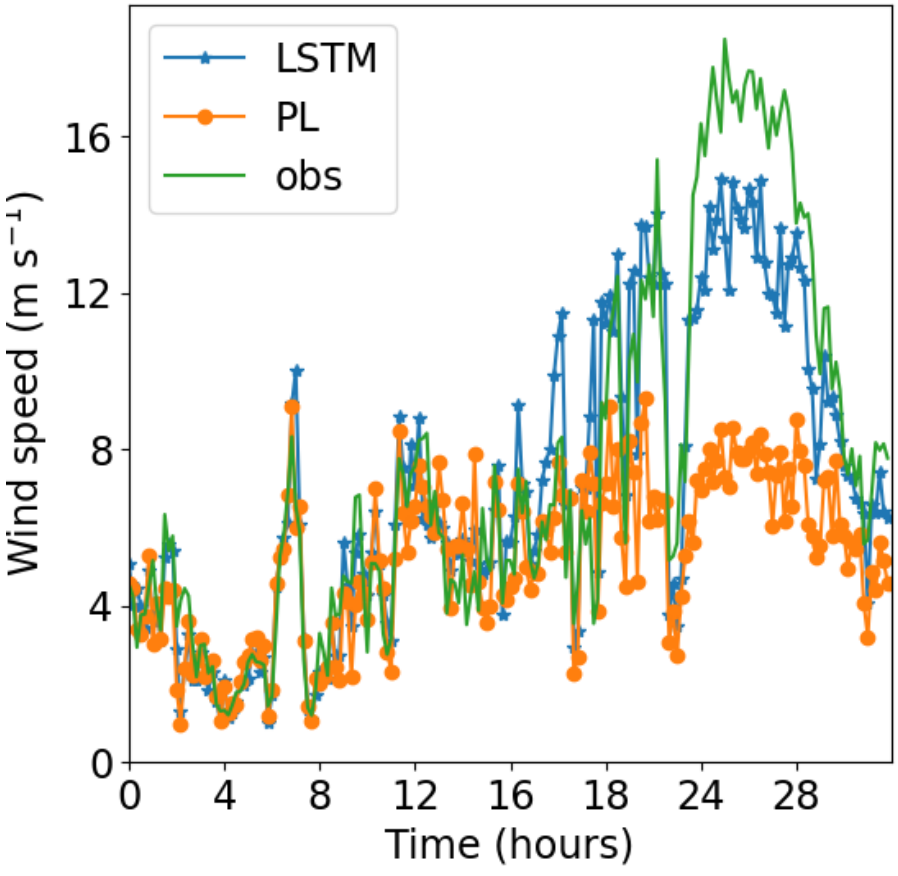

Figure 11. Site 2: 160 m wind speed temporal series (**Experiment 1**)

https://doi.org/10.5194/wes-2023-104
Preprint. Discussion started: 9 October 2023

eawe european academy of wind energy
Open Access WIND ENERGY SCIENCE DISCUSSIONS

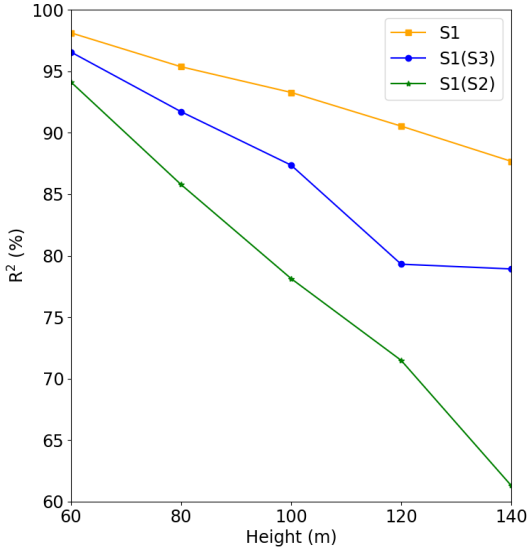

Figure 12. Comparison between the **Experiment 1** and **Experiment 3**, where S1 is the result of the Experiment 1; S1(S2) is the forecast for the Site 1 ran with the model of the Site 2; and S1(S3) is the forecast for the Site 1 ran with the model of the Site 3

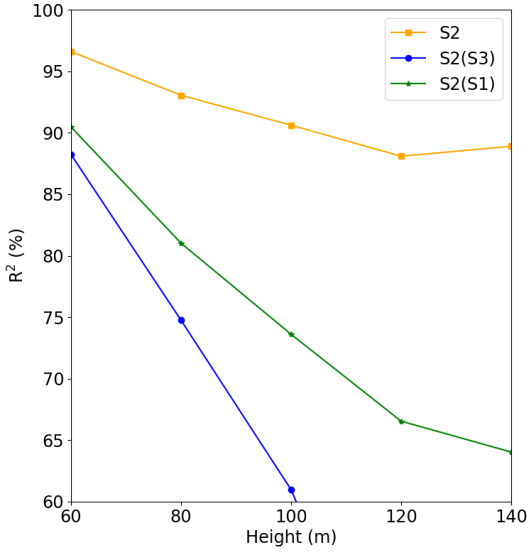

Figure 13. Comparison between the **Experiment 1** and **Experiment 3**, where S2 is the result of the Experiment 1; S2(S1) is the forecast for the Site 2 ran with the model of the Site 1; and S2(S3) is the forecast for the Site 2 ran with the model of the Site 3

https://doi.org/10.5194/wes-2023-104
Preprint. Discussion started: 9 October 2023

eawe european academy of wind energy
Open Access WIND ENERGY SCIENCE DISCUSSIONS

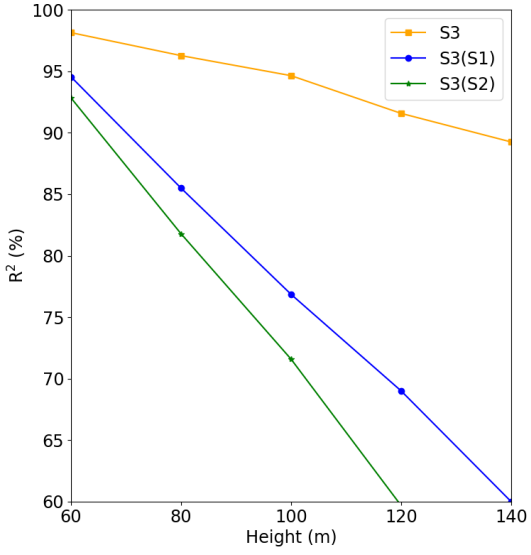

Figure 14. Comparison between the **Experiment 1** and **Experiment 3**, where S3 is the result of the Experiment 1; S3(S1) is the forecast for the Site 3 ran with the model of the Site 1; and S3(S2) is the forecast for the Site 3 ran with the model of the Site 1

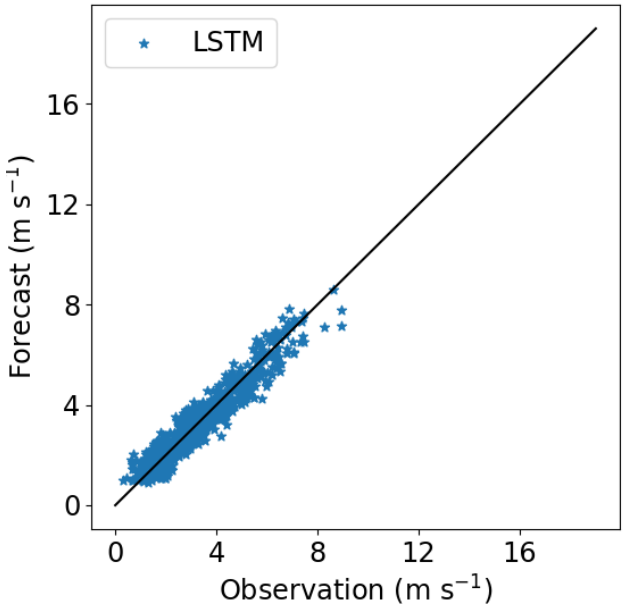

Figure 15. Correlation between forecasted and observed data for the Site 1 with the model trained at Site 3. Height: 80 m

https://doi.org/10.5194/wes-2023-104
Preprint. Discussion started: 9 October 2023

eawe european academy of wind energy
Open Access WIND ENERGY SCIENCE DISCUSSIONS

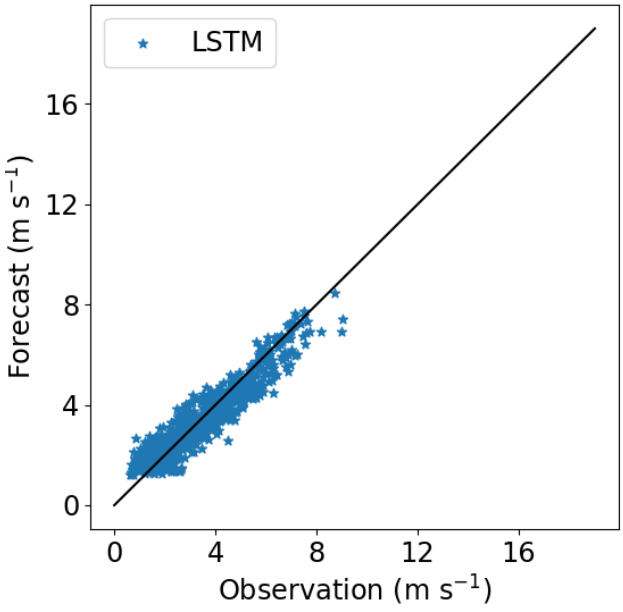

Figure 16. Correlation between forecasted and observed data for the Site 1 with the model trained at Site 3. Height: 100 m

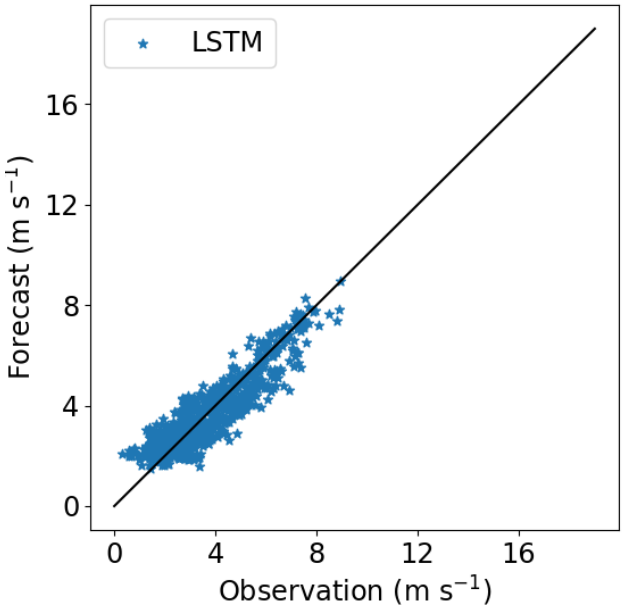

Figure 17. Correlation between forecasted and observed data for the Site 1 with the model trained at Site 3. Height: 140 m

https://doi.org/10.5194/wes-2023-104
Preprint. Discussion started: 9 October 2023

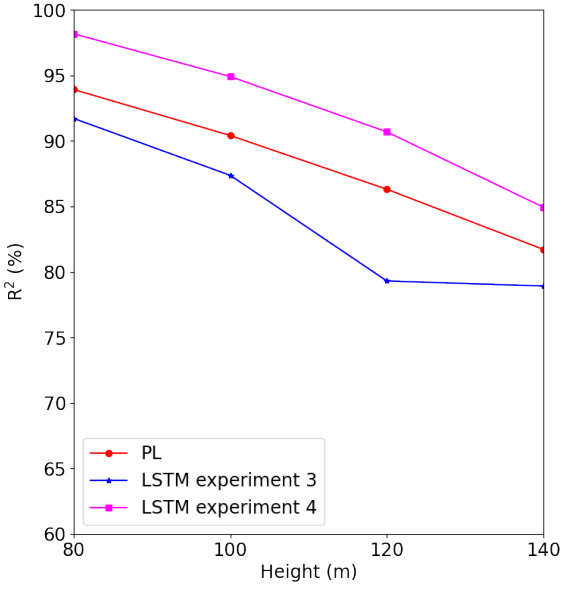

Figure 18. Site 1: Comparison for the **PL**, **Experiment 3** and **Experiment 4** estimates

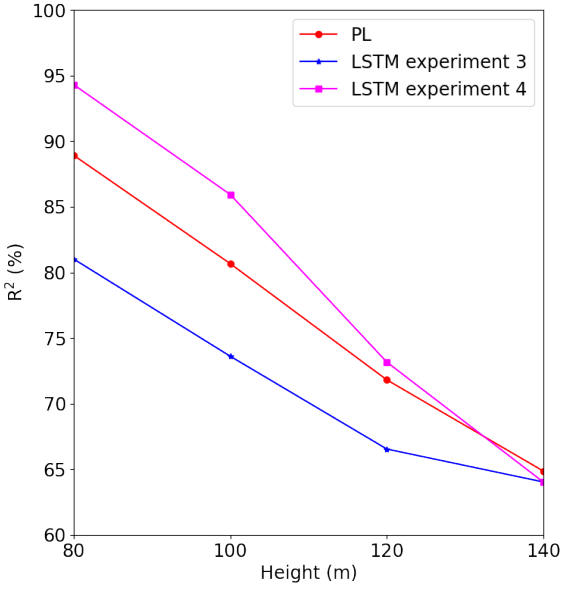

Figure 19. Site 2: Comparison for the **PL**, **Experiment 3** and **Experiment 4** estimates

https://doi.org/10.5194/wes-2023-104
Preprint. Discussion started: 9 October 2023

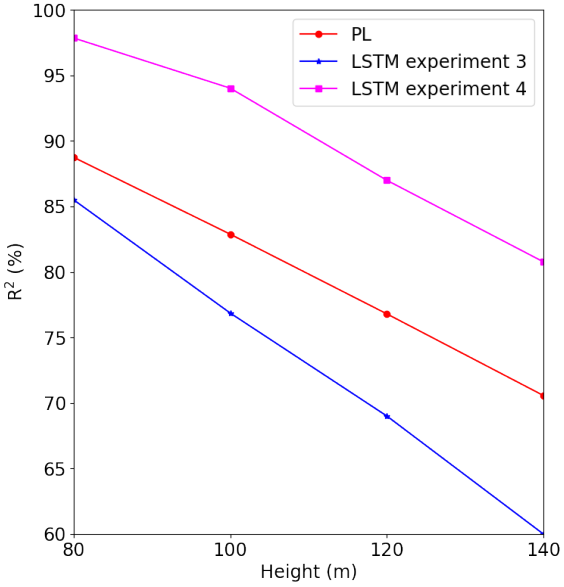

Figure 20. Site 3: Comparison for the **PL**, **Experiment 3** and **Experiment 4** estimates

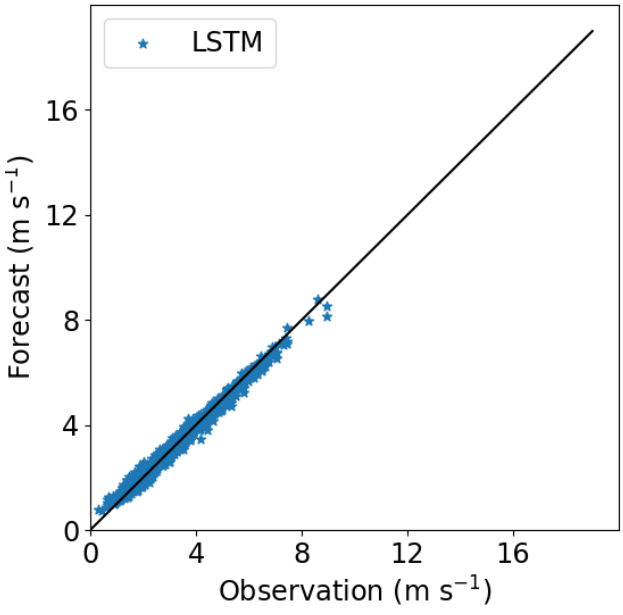

Figure 21. As Fig. 15, except the 60 m wind speed was added to the input dataset

https://doi.org/10.5194/wes-2023-104
Preprint. Discussion started: 9 October 2023

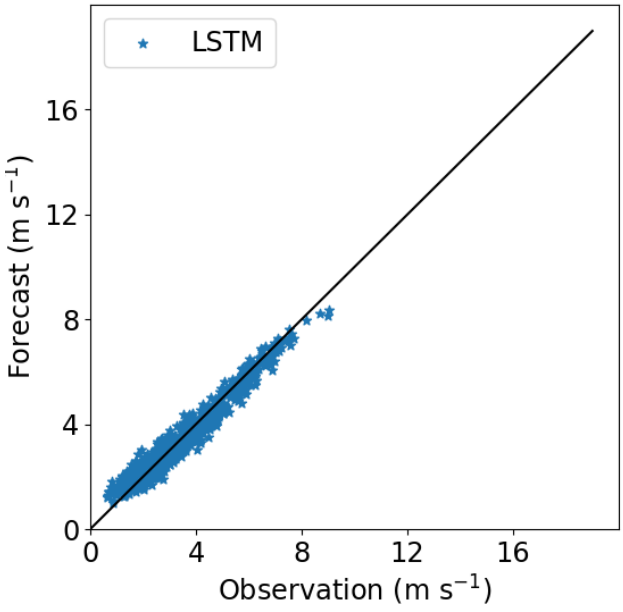

Figure 22. As Fig. 16, except the 60 m wind speed was added to the input dataset

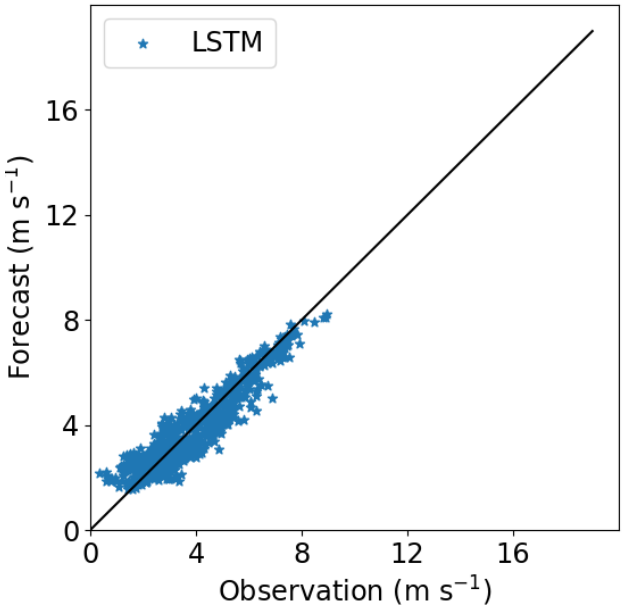

Figure 23. As Fig. 17, except the 60 m wind speed was added to the input dataset

https://doi.org/10.5194/wes-2023-104
Preprint. Discussion started: 9 October 2023

eawe european academy of wind energy
Open Access WIND ENERGY SCIENCE DISCUSSIONS

4 Conclusions

Nowadays, the machine learning techniques produce successfully results to forecast environmental processes. However, forecasting the wind speed is still a challenge due its randomly nature and researchers are dedicating considerable time and efforts to reach confident results. Comparative studies showed the superiority of the LSTM to forecast the wind speed against other machine learning techniques. Adding more meteorological variables has also improved the results. Ensemble and hybrid methods are strategies that also contribute to the model performances.

Only recently, the machine learning techniques have been applied to extrapolate the wind speed to higher heights. The models generally require large datasets with some observational heights. After testing some commonly used algorithms for the wind speed forecast (Random Forest Trees, Support Vector Regression and Multi-layer Perceptron), we found out the LSTM outperformed all of them. The LSTM outperformed even the decomposition methods.

We also evaluated different dataset sizes and found out that the model didn´t improve even if the dataset size increases beyond that presented in Table A1; however, the model is sensitive to the training data percentage. In this study, taking 90% of the dataset for training produced the best result. The tests also showed best results for 10-min mean as input data than for 30-min or 1-hour mean.

Including the 40 m wind direction, TKE and the hour to the input dataset improved the model, which outperformed the Power Law as the distance from the surface increases. Adding the 60 m wind speed observations to the dataset improved the results, as expected from results of previous studies. However, the improvement was better to the Sites 1 and 2 than for the Site 3. The causes should be investigated in a future work.

Even over complex terrain and with a relatively short dataset (an observational campaign shorter than 3 months), the LSTM outperformed the Power Law. The Power Law cannot reproduce features like the LLJs that are often observed, at least over the Sites 1 and 3. The Site 2 is strongly influenced by the sea and land breezes and the LSTM model captured the abrupt changes of the wind profile better than the Power Law.

Considering that the energy transition is a need and the wind potential is still unknown, it is motivating found out that a short observational campaign produces such good results, despite of the high cost of the Doppler lidar. This can awake the stakeholders to acquire Doppler lidars and to develop cooperative studies or consortiums as strategy to leverage the wind potential evaluation, since the Doppler lidars are mobile systems and easily operated.

As future work, we expect to test the LSTM recurrent neural network, but providing 1 min or 5 min means observational data as input instead of 10 min mean. This will require a new observational campaign. We would also like to evaluate if providing more observational data as surface pressure and surface temperature would improve the results.

Code and data availability. Algorithms and data are available under request. Please, contact cassia.beu@gmail.com

https://doi.org/10.5194/wes-2023-104
Preprint. Discussion started: 9 October 2023

eawe european academy of wind energy
Open Access WIND ENERGY SCIENCE DISCUSSIONS

Appendix A

Table A1. Dataset size and hyperparameters

			Experiment 1			Experiment 2		
site	data points	Training data (%)	units	epochs	batch size	units	epochs	batch size
1	10000	90	30	30	2	30	30	2
2	12000	90	20	20	2	15	30	2
3	8000	90	50	150	2	20	70	2

Author contributions. The authors contributed equally to this work.

Competing interests. There are no competing of interests.

Acknowledgements. The authors acknowledge the Instituto Nacional de Pesquisas Energéticas (IPEN) and the Financiadora de Estudos e Projetos (FINEP).

https://doi.org/10.5194/wes-2023-104
Preprint. Discussion started: 9 October 2023

eawe european academy of wind energy
Open Access WIND ENERGY SCIENCE DISCUSSIONS

References

Al-Shaikhi, A., Nuha, H., Mohandes, M., Rehman, S., and Adrian, M.: Vertical wind speed extrapolation model using long short-term memory and particle swarm optimization, Energy Science & Engineering, 10, 4580–4594, https://doi.org/10.1002/ese3.1291, 2022.

Bali, V., Kumar, A., and Gangwar, S.: Deep Learning based Wind Speed Forecasting-A Review, in: 2019 9th International Conference on Cloud Computing, Data Science & Engineering (Confluence), IEEE, https://doi.org/10.1109/confluence.2019.8776923, 2019.

Baquero, L., Torio, H., and Leask, P.: Machine Learning Algorithms for Vertical Wind Speed Data Extrapolation: Comparison and Performance Using Mesoscale and Measured Site Data, Energies, 15, 5518, https://doi.org/10.3390/en15155518, 2022.

Beu, C. M. L. and Landulfo, E.: Turbulence Kinetic Energy Dissipation Rate Estimate for a Low-Level Jet with Doppler Lidar Data: A Case Study, Earth Interactions, 26, 112–121, https://doi.org/10.1175/ei-d-20-0027.1, 2022.

Bodini, N. and Optis, M.: The importance of round-robin validation when assessing machine-learning-based vertical extrapolation of wind speeds, Wind Energy Science, 5, 489–501, https://doi.org/10.5194/wes-5-489-2020, 2020a.

Bodini, N. and Optis, M.: How accurate is a machine learning-based wind speed extrapolation under a round-robin approach?, Journal of Physics: Conference Series, 1618, 062 037, https://doi.org/10.1088/1742-6596/1618/6/062037, 2020b.

Cabral, V., Reis, F., Veloso, V., Correa, C., Kuhn, C., and Zarfl, C.: The consequences of debris flows in Brazil: a historical analysis based on recorded events in the last 100 years, Landslides, 20, 511–529, https://doi.org/10.1007/s10346-022-01984-7, 2022.

Cheng, C.-H. and Tsai, M.-C.: An Intelligent Time Series Model Based on Hybrid Methodology for Forecasting Concentrations of Significant Air Pollutants, Atmosphere, 13, 1055, https://doi.org/10.3390/atmos13071055, 2022.

Dalton, A. and Bekker, B.: Exogenous atmospheric variables as wind speed predictors in machine learning, Applied Energy, 319, 119 257, https://doi.org/10.1016/j.apenergy.2022.119257, 2022.

de Oliveira, A. P., Degrazia, G. A., Moraes, O. L. L., and Tirabassi, T.: Numerical Study of the Nocturnal Planetary Boundary Layer at Low Latitutes, Transactions on Ecology and the Environment, 6, 167–174, 1995.

Gasparoto, E. A. G., Tonello, K. C., Shinzato, E. T., and de Oliveira Averna Valente, R.: Throughfall in different forest stands of Iperó, São Paulo, CERNE, 20, 303–310, https://doi.org/10.1590/01047760.201420021260, 2014.

He, J., Yang, H., Zhou, S., Chen, J., and Chen, M.: A Dual-Attention-Mechanism Multi-Channel Convolutional LSTM for Short-Term Wind Speed Prediction, Atmosphere, 14, 71, https://doi.org/10.3390/atmos14010071, 2022.

Hogan, D. J.: Population, Poverty and Pollution in Cubatao, Sao Paulo, in: Population and Environment in Industrialized Regions, Polish Academy of Sciences, 1994.

Jesemann, A.-S., Matthias, V., Böhner, J., and Bechtel, B.: Using Neural Network NO2-Predictions to Understand Air Quality Changes in Urban Areas—A Case Study in Hamburg, Atmosphere, 13, 1929, https://doi.org/10.3390/atmos13111929, 2022.

Jiang, H., Wang, X., and Sun, C.: Predicting PM2.5 in the Northeast China Heavy Industrial Zone: A Semi-Supervised Learning with Spatiotemporal Features, Atmosphere, 13, 1744, https://doi.org/10.3390/atmos13111744, 2022.

Keras: Kerasguide, https://keras.io/api/layers/recurrent_layers/lstm/, 2023.

Klockow, D. and Targa, H. J.: Performance and results of a six-year German/Brazilian research project in the industrial area of Cubatão/SP Brazil, Pure and Applied Chemistry, 70, 2287–2293, https://doi.org/10.1351/pac199870122287, 1998.

Lemos, M. C. D. M.: The Cubatão Pollution Control Project: Popular Participation and Public Accountability, The Journal of Environment & Development, 7, 60–76, https://doi.org/10.1177/107049659800700105, 1998.

https://doi.org/10.5194/wes-2023-104
Preprint. Discussion started: 9 October 2023

Liu, Y., Cai, J., and Tan, G.: Multi-Level Circulation Pattern Classification Based on the Transfer Learning CNN Network, Atmosphere, 13, 1861, https://doi.org/10.3390/atmos13111861, 2022.

Medsker, L. and Jain, L. C., eds.: Recurrent Neural Networks, CRC Press, https://doi.org/10.1201/9781420049176, 1999.

Mohandes, M. A. and Rehman, S.: Wind Speed Extrapolation Using Machine Learning Methods and LiDAR Measurements, IEEE Access, 6, 77 634–77 642, https://doi.org/10.1109/access.2018.2883677, 2018.

Morellato, L. P. C. and Haddad, C. F. B.: Introduction: The Brazilian Atlantic Forest1, Biotropica, 32, 786–792, https://doi.org/10.1111/j.1744-7429.2000.tb00618.x, 2000.

Mustakim, R., Mamat, M., and Yew, H. T.: Towards On-Site Implementation of Multi-Step Air Pollutant Index Prediction in Malaysia Industrial Area: Comparing the NARX Neural Network and Support Vector Regression, Atmosphere, 13, 1787, https://doi.org/10.3390/atmos13111787, 2022.

Musyimi, P. K., Sahbeni, G., Timár, G., Weidinger, T., and Székely, B.: Actual Evapotranspiration Estimation Using Sentinel-1 SAR and Sentinel-3 SLSTR Data Combined with a Gradient Boosting Machine Model in Busia County, Western Kenya, Atmosphere, 13, 1927, https://doi.org/10.3390/atmos13111927, 2022.

Nuha, H., Mohandes, M., Rehman, S., and A-Shaikhi, A.: Vertical wind speed extrapolation using regularized extreme learning machine, FME Transactions, 50, 412–421, https://doi.org/10.5937/fme2203412n, 2022.

O'Malley, T., Bursztein, E., Long, J., Chollet, F., Jin, H., Invernizzi, L., et al.: KerasTuner, https://github.com/keras-team/keras-tuner, 2019.

Pedregosa, F., Varoquaux, G., Gramfort, A., Michel, Grisel, O., Blondel, M., Prettenhofer, Dubourg, V., Vanderplas, J., Passos, Brucher, M., Perrot, M., and Duchesnay, E.: Scikit-learn: Machine Learning in Python, Journal of Machine Learning Research, 12, 2825–2830, 2011.

Pintor, A., Pinto, C., Mendonca, J., Pilao, R., and Pinto, P.: Insights on the use of wind speed vertical extrapolation methods, in: 20th International Conference on Renewable Energies and Power Quality, RE & PQJ, 2022.

Ribeiro, F. N., de Oliveira, A. P., Soares, J., de Miranda, R. M., Barlage, M., and Chen, F.: Effect of sea breeze propagation on the urban boundary layer of the metropolitan region of Sao Paulo, Brazil, Atmospheric Research, 214, 174–188, https://doi.org/10.1016/j.atmosres.2018.07.015, 2018.

Sánchez, M. P., de Oliveira, A. P., Varona, R. P., Tito, J. V., Codato, G., Ynoue, R. Y., Ribeiro, F. N. D., Filho, E. P. M., and da Silveira, L. C.: Observational Investigation of the Low-Level Jets in the Metropolitan Region of São Paulo, Brazil, Earth and Space Science, 9, https://doi.org/10.1029/2021ea002190, 2022.

Sherstinsky, A.: Fundamentals of Recurrent Neural Network (RNN) and Long Short-Term Memory (LSTM) network, Physica D: Nonlinear Phenomena, 404, 132 306, https://doi.org/10.1016/j.physd.2019.132306, 2020.

Smagulova, K. and James, A. P.: A survey on LSTM memristive neural network architectures and applications, The European Physical Journal Special Topics, 228, 2313–2324, https://doi.org/10.1140/epjst/e2019-900046-x, 2019.

Song, Y. and Wang, Y.: Global Wildfire Outlook Forecast with Neural Networks, Remote Sensing, 12, 2246, https://doi.org/10.3390/rs12142246, 2020.

Soria-Ruiz, J., Fernandez-Ordoñez, Y. M., Ambrosio-Ambrosio, J. P., Escalona-Maurice, M. J., Medina-García, G., Sotelo-Ruiz, E. D., and Ramirez-Guzman, M. E.: Flooded Extent and Depth Analysis Using Optical and SAR Remote Sensing with Machine Learning Algorithms, Atmosphere, 13, 1852, https://doi.org/10.3390/atmos13111852, 2022.

Stull, R. B., ed.: An Introduction to Boundary Layer Meteorology, Springer Netherlands, https://doi.org/10.1007/978-94-009-3027-8, 1988.

https://doi.org/10.5194/wes-2023-104
Preprint. Discussion started: 9 October 2023

Tukur, A., Chidiebere, O., Shittu, F., and Lawal Abdulrahman, M.: Neural Network Ensemble for Medium Term Forecast of Wind Power Generation: A Review Keyword: Artificial Neural Network, Ensemble technique, Recurrent Neural Network, Deep Learning and Deep Recurrent neural Network, International Journal Of Advance Research And Innovative Ideas In Education, 8, 2022, 2022.

Türkan, Y. S., Aydoğmuş, H. Y., and Erdal, H.: The prediction of the wind speed at different heights by machine learning methods, An International Journal of Optimization and Control: Theories & Applications (IJOCTA), 6, 179–187, https://doi.org/10.11121/ijocta.01.2016.00315, 2016.

Vassallo, D., Krishnamurthy, R., and Fernando, H. J. S.: Decreasing wind speed extrapolation error via domain-specific feature extraction and selection, Wind Energy Science, 5, 959–975, https://doi.org/10.5194/wes-5-959-2020, 2020.

Vieira, B. C. and Gramani, M. F.: Serra do Mar: The Most "Tormented" Relief in Brazil, in: World Geomorphological Landscapes, pp. 285–297, Springer Netherlands, https://doi.org/10.1007/978-94-017-8023-0_26, 2015.

Vieira-Filho, M. S., Lehmann, C., and Fornaro, A.: Influence of local sources and topography on air quality and rainwater composition in Cubatão and São Paulo, Brazil, Atmospheric Environment, 101, 200–208, https://doi.org/10.1016/j.atmosenv.2014.11.025, 2015.

Wang, J., Li, Q., and Zeng, B.: Multi-layer cooperative combined forecasting system for short-term wind speed forecasting, Sustainable Energy Technologies and Assessments, 43, 100 946, https://doi.org/10.1016/j.seta.2020.100946, 2021.

Yu, Y., Si, X., Hu, C., and Zhang, J.: A Review of Recurrent Neural Networks: LSTM Cells and Network Architectures, Neural Computation, 31, 1235–1270, https://doi.org/10.1162/neco_a_01199, 2019.

Zhang, Y., Wang, Y., Zhu, Y., Yang, L., Ge, L., and Luo, C.: Visibility Prediction Based on Machine Learning Algorithms, Atmosphere, 13, 1125, https://doi.org/10.3390/atmos13071125, 2022.

Zhou, F., Huang, Z., and Zhang, C.: Carbon price forecasting based on CEEMDAN and LSTM, Applied Energy, 311, 118 601, https://doi.org/10.1016/j.apenergy.2022.118601, 2022.

Zhou, J., Feng, J., Zhou, X., Li, Y., and Zhu, F.: Estimating Site-Specific Wind Speeds Using Gridded Data: A Comparison of Multiple Machine Learning Models, Atmosphere, 14, 142, https://doi.org/10.3390/atmos14010142, 2023.